Available online at www.sciencedirect.com

ScienceDirect

Physics Procedia 64 (2015) 177 – 182

Physics Procedia

Scientific Workshop on Nuclear Fission dynamics and the Emission of Prompt Neutrons and Gamma Rays, THEORY-3

Neutron-induced fission cross section of ^{240,242}Pu

P. Salvador-Castiñeira[a,b,*], T. Bryś[a], R. Eykens[a], F.-J. Hambsch[a], A. Göök[a], S. Oberstedt[a], C. Pretel[b], G. Sibbens[a], D. Vanleeuw[a], M. Vidali[a]

[a]*European Commission - Joint Research Centre - Institute for Reference Materials and Measurements, Retieseweg 111, B-2440 Geel, Belgium*
[b]*Institute of Energy Technologies, Technical University of Catalonia, Avda. Diagonal 647, E-08028 Barcelona, Spain*

Abstract

A sensitivity analysis for the new generation of fast reactors [Salvatores (2008)] has shown the importance of improved cross section data for several actinides. Among them, the ^{240,242}Pu(n,f) cross sections require an accuracy improvement to 1-3% and 3-5%, respectively, from the current level of 6% and 20%. At the Van de Graaff facility of the Institute for Reference Materials and Measurements (JRC-IRMM) the fission cross section of the two isotopes was measured relative to two secondary standard reactions, ^{237}Np(n,f) and ^{238}U(n,f), using a twin Frisch-grid ionization chamber. The secondary standard reactions were benchmarked through measurements against the primary standard reaction ^{235}U(n,f) in the same geometry. Sample masses were determined by means of low-geometry alpha counting or/and a 2π Frisch-grid ionization chamber, with an uncertainty lower than 2%. The neutron flux and the impact of scattering from material between source and target was examined, the largest effect having been found in cross section ratio measurements between a fissile and a fertile isotope. Our ^{240,242}Pu(n,f) cross sections are in agreement with previous experimental results and slightly lower than present evaluations. In case of the ^{242}Pu(n,f) reaction no evidence for a resonance at E_n=1.1 MeV was found.

Peer-review under responsibility of the European Commission, Joint Research Centre – Institute for Reference Materials and Measurements

Keywords: neutron-induced fission cross section; ^{240}Pu(n,f); ^{242}Pu(n,f); ^{237}Np(n,f); ^{238}U(n,f)

1. Introduction

For the design of the new Generation-IV nuclear power plants the accuracy of several nuclear data needs to be improved in certain energy regions. A report issued by the OECD Nuclear Energy Agency [Salvatores (2008)] pointed out the most relevant nuclear data needs for fast reactors, not only related with the reactor core but, additionally, related with structural materials. Within this list the neutron-induced fission cross sections of ^{240,242}Pu were requested to be improved from the current uncertainty of 6% for ^{240}Pu and 20% for ^{242}Pu to a target accuracy within 1-3% and 3-5%, respectively.

* Corresponding author.
E-mail address: paula.salvador@upf.edu

Peer-review under responsibility of the European Commission, Joint Research Centre – Institute for Reference Materials and Measurements
doi:10.1016/j.phpro.2015.04.024

Table 1. Description of the samples under study (^{240,242}Pu) and the reference samples used (^{237}Np, ^{238}U and ^{235}U) [Pommé (2012); Sibbens (2014)].

	^{240}Pu	^{242}Pu	^{237}Np	^{235}U	^{238}U
Method	electrodeposition			vacuum deposition	
Mass[a] (μg)	93 (.4%)	671 (.9%)	390 (.3%)	584 (2%)	577 (.4%)
Diameter (mm)	30 (.1%)	30 (.1%)	12.7	28	30
Areal density (μg/cm^2)	13.19 (.4%)	95.3 (.8%)	308 (.3%)	94.8 (2%)	81.7 (.4%)
Backing	Aluminum	Aluminum	Stainless steel		Transparent
α-activity (MBq)	0.780 (.4%)	0.095 (.3%)	0.001 (.1%)	265.7 Bq (2%)[b]	7 Bq (.5%)
%^{238}Pu	0.0733	0.0027	99.8% ^{237}Np	99.5% ^{235}U	99.99% ^{238}U
%^{239}Pu	0.0144	0.0044	0.2% ^{238}Pu	0.2% ^{234}U	<0.02% ^{234}U
%^{240}Pu	99.8915	0.0192		0.03% ^{236}U	
%^{241}Pu	0.0041	0.0081		0.3% ^{238}U	
%^{242}Pu	0.0203	99.9652			
%^{244}Pu	0.0001	0.0004			

[a] The sample mass corresponds just to the main isotope and not to the total mass of the chemical compound.
[b] The sample activity of ^{235}U sample considers the contribution of the ^{234}U and ^{235}U isotopes.

To address some of the needs for the development of the future nuclear power reactors and their corresponding fuel cycles the ANDES collaboration (Accurate Nuclear Data for nuclear Energy Sustainability) [ANDES (2010)] developed a program of specifically targeted actions. The present work, as part of this collaboration, provides new fission cross section data for ^{240}Pu(n,f) and ^{242}Pu(n,f). The fission cross section of the two isotopes was measured relative to two secondary standard reactions, ^{237}Np(n,f) and ^{238}U(n,f), using a twin Frisch-grid ionization chamber. The secondary standard reactions were benchmarked through measurements against the primary standard reaction ^{235}U(n,f) in the same geometry. Finally, a detailed study of the necessary corrections to our cross section data was carried out, too.

2. Experimental setup

At the Van de Graaff accelerator of the JRC-IRMM protons were accelerated to produce a quasi-monoenergetic neutron beam through two different reactions: ^{7}Li(p,n)^{7}Be and T(p,n)^{3}He. The neutron energy range between 0.3 and 3 MeV was covered. A Twin Frisch-Grid Ionization Chamber (TFGIC) was used as fission fragment detector. As counting gas, P10 gas (90% Ar + 10% CH_4) was used first and later replaced by CH_4, at a constant flow rate of ca. 50 ml/min (100 ml/min when using CH_4) and a pressure of 105 kPa. A schematic drawing of the setup may be found elsewhere [Salvador-Castiñeira (2014)]. The five electrodes of the TFGIC (two anodes, two grids and a cathode) were connected to charge-sensitive pre-amplifiers. The output signals were fed into 12-bit wave-form digitizers (WFD) with a sampling speed of 100 Ms/s. The cathode signal was used as trigger after treated with a Timing Filter Amplifier (TFA) and a Constant Fraction Discriminator (CFD), where an electronic threshold was set for rejecting α-particles. The recorded signal traces were stored and processed offline using a root-based digital signal processing (DSP) library [ROOT (2014)].

The plutonium and the standard isotope samples were produced by the target preparation group of JRC-IRMM. Table 1 provides an extended description of the samples. The mass of the ^{240}Pu sample was chosen to minimize its α-activity. The mass of all the samples were measured by means of low geometry α-counting, reaching uncertainties below 1% for all samples, but for ^{235}U. The high uncertainty on the ^{235}U sample mass is due to the complexity of the α-branching of this isotope. Additionally, the ^{238}U and the ^{235}U sample were measured again using a Single Frisch-Grid Ionization Chamber, obtaining results within uncertainties compared with the low geometry α-counting method.

A study of the homogeneity of the ^{237}Np and ^{240,242}Pu samples was performed doing a scan of the α-activity of the sample at different places on its surface. Results showed that the vacuum deposited samples (i.e. ^{237}Np) have a very high homogeneity, whilst the electrodeposited ones (i.e. ^{240,242}Pu) have an increased density of mass in the outer diameter. For the ^{240}Pu the outer diameter has on average 11.4% higher mass density than the inner one. In the case of ^{242}Pu the outer diameter has 7.4% higher mass density than the inner one.

3. Fission cross section measurements

Several measurement campaigns were performed. The ratios measured were ^{240,242}Pu(n,f)/^{237}Np(n,f), ^{240,242}Pu(n,f)/^{235}U(n,f), ^{237}Np(n,f)/^{235}U(n,f), ^{238}U(n,f)/^{235}U(n,f), ^{240,242}Pu(n,f)/^{238}U(n,f) and ^{237}Np(n,f)/^{238}U(n,f).

The neutron-induced fission cross section was calculated as

$$\sigma^S_{main,0} = \frac{C_S}{C_R}\frac{F_S}{F_R}\cdot\left(\sum_i \frac{N^R_i}{N^S_{main}}\frac{\Phi^R_0}{\Phi^S_0}\sigma^R_{i,0} + \sum_i \frac{N^R_i}{N^S_{main}}\frac{\Phi^R_1}{\Phi^S_0}\sigma^R_{i,1}\right) - \sum_i \frac{N^S_i}{N^S_{main}}\frac{\Phi^S_1}{\Phi^S_0}\sigma^S_{i,1} - \sum_j \frac{N^S_j}{N^S_{main}}\sigma^S_{j,0} \quad (1)$$

where the index *main* accounts for the main isotope of the sample (S), R refers to the reference sample, C_i is the net count rate described as $C = \frac{C_{total}}{\epsilon} - \sum_i C_{SF,i}$, F_i are the correction factors due to the energy distribution of the neutrons calculated using MCNP (2014), N are the number of atoms, Φ^R/Φ^S is the ratio of neutron flux due to the difference of sample spot size and homogeneity, the subindexes 0 and 1 refer to the ground state and excited state of the ^{7}Li(p,n)^{7}Be reaction, respectively. The excited state of the recoil nucleus of the ^{7}Li(p,n)^{7}Be reaction starts at ≈0.7 MeV and has around 0.4 MeV less energy than the ground state. The differential cross section of the excited state is at least one order of magnitude lower than the ground state and its corresponding correction is below 1%. The correction due to the sample spot size and homogeneity is below 3%.

The spontaneous fission counts (C_{SF}) were calculated using the fission half-lives obtained for ^{240,242}Pu in Salvador-Castiñeira (2013). The efficiency (ϵ) included the effects of anisotropy of the fission fragment distribution, the neutron momentum transfer and the thickness of the sample; additionally, the position of the target relative to the neutron beam (down- or up-stream) was accounted for [Carlson (1974)].

One of the most relevant correction to be applied was the interaction of the neutron beam with the matter between the neutron producing target and the deposits inside the TFGIC. This interaction was studied carefully by means of MCNP calculations and will be explained hereafter.

3.1. Neutron background correction

A non-desirable neutron background was generated through inelastic scattering on material in between the neutron production target and the sample deposits as well as by neutron returning from the walls (room-return). Two setup configurations were used during the experiments. The first one consisted mainly of a neutron producing target cooled by 2 mm of water and, at 7 cm distance, the samples were placed at the center of the TFGIC. The second configuration consisted of a water layer of 1 mm and, additionally, the TFGIC and part of the beam line were shielded by a B_4C-paraffin cage. The latter configuration was used when the ^{235}U reference sample was employed to prevent thermalized neutrons from room-return to induce fission in ^{235}U.

The neutron energy distribution, its emission angle and emission probability entered the simulations according to the tables in Liskien (1973, 1975). The result of the simulation was the average flux over the sample surface as a function of the incident neutron energy normalized by the neutron-induced fission cross section of the corresponding isotope. The influence of the thermalized neutron background was more severe when a fissile isotope (i.e. ^{235}U) was used. In addition, the correction factors were higher for the first setup configuration since the water layer was thicker.

3.2. Sources of uncertainty

The uncertainties related to the experiment are listed in Table 2. The largest contribution to the uncertainty is due to the ^{235}U mass uncertainty (when the cross section is normalized to this standard), the ENDF/B-VII.1 (2011) evaluation for the ^{237}Np(n,f) cross section, when used, the efficiency uncertainty and the spontaneous fission rate uncertainty. The total uncertainty for each ratio measurement is lower than 3% in cases where the reference cross section was ^{235}U(n,f) or ^{238}U(n,f). In the case of a normalization with the ^{237}Np(n,f) cross section the total uncertainty is close to 5%. The statistical uncertainty is, in most of individual data sets, around 0.5%, except for a single case where it amounts to 1.4%.

Table 2. Summary of the systematic uncertainties corresponding to the cross section measurements.

Uncertainty source	^{238}U	^{237}Np	^{240}Pu	^{242}Pu
Statistical	0.5%	0.5%	0.5%	<0.5%
Counts SF	-	-	<1.1%	<1.3%
Sample Mass	0.5%	0.3%	0.4%	0.9%
Reference sample ^{235}U mass	1.5% (samples #2 & #6)		2% (sample #1)[a]	
Efficiency	1%	1%	1%	1%
Sample purity	0.001%	0.001%	0.001%	0.001%
Correction of neutron spectrum	<0.2%	<0.2%	<0.1%	<0.1%
MCNP corrections (ratio)	0.5%	0.5%	0.5%	0.5%
^{237}Np - ENDF	2.2-4%			
^{238}U - standard	0.7%			
^{235}U - standard	< 0.8%			

[a] Three different ^{235}U samples were used. For simplicity in Table 1 just one of them was described.

4. Results and discussions

4.1. ^{238}*U(n,f) cross section*

The ^{238}U(n,f) cross section was measured relative to ^{235}U(n,f). Figure 1 presents the results obtained after applying all the corrections described above (red crosses). The ENDF/B-VII.1 (2011), JEFF 3.2 (2009) and JENDL 4.0 (1995) are plotted. The results of this experiment are 10% lower than the ENDF/B-VII.1 evaluation and 10% higher than the JEFF 3.2 at the threshold region (around 1.6 MeV). Nevertheless, at the plateau region, the present data is in good agreement with the JEFF 3.2 evaluation and the previous data of Lamphere (1956); and 6% higher than the ENDF/B-VII.1 evaluation.

4.2. ^{237}*Np(n,f) cross section*

Three sets of measurements were performed to determine the ^{237}Np(n,f) cross section. First, the ^{238}U(n,f) cross section was used as reference in two configurations: with and without shielding. The results achieved were within uncertainties. Then, a measurement with the shielding configuration and using the ^{235}U(n,f) cross section as reference was done, first, using a LiF neutron producing target (from 0.5 MeV up to 1.8 MeV) and, second, using a TiT neutron producing target (from 1.6 MeV up to 3 MeV). The results normalized to ^{238}U(n,f) showed a 5-7% higher cross section than the present evaluations and in good agreement with the results of Paradela et al. (2010). Additionally, the results normalized with the ^{235}U(n,f) cross section and using the TiT neutron producing target were in agreement with the ones normalized to ^{238}U(n,f). Nevertheless, when using the LiF neutron producing target and the ^{235}U(n,f) cross section the results obtained were in concordance with the present evaluations, thus 5% lower than the cross section obtained at 1.6 MeV and 1.8 MeV when using the TiT target.

In Figure 1 two weighted averages of the three data sets are shown. In first place, the weighted average was done with all the above data sets normalized using the ENDF/B-VII.1 evaluation (red crosses). In second place, the weighted average was calculated after normalizing the ^{238}U(n,f) data set to the cross section obtained in the previous subsection (green stars).

4.3. ^{240}*Pu(n,f) cross section*

In the case of ^{240}Pu(n,f) three different measurements were done. The first two using the setup without shielding and relative to ^{237}Np(n,f) (using a LiF neutron producing target) and relative to ^{238}U(n,f) (using a TiT target). The third measurement was done with the shielding configuration and using as reference ^{235}U(n,f) (with a LiF target). The data taken at the threshold region is in agreement with the present evaluations, either using ^{237}Np(n,f) as reference or ^{235}U(n,f). At the plateau region all the sets are around 2-5% lower than the evaluations. When using the ^{238}U(n,f) cross section as reference at 1.6 MeV and 1.7 MeV the cross section shape of the data set was not resembling the evaluations, a similar effect was observed at the same energies with the results obtained with the ratio ^{237}Np(n,f)/^{238}U(n,f).

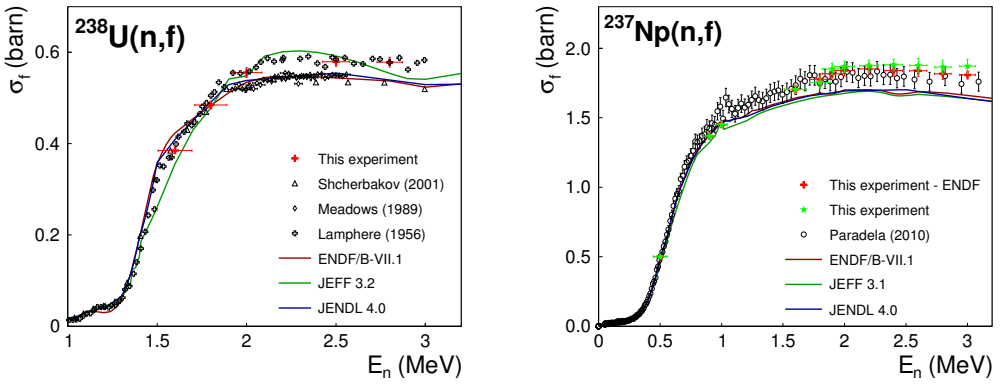

Fig. 1. Summary of the results achieved for the neutron-induced fission cross section of ^{238}U (left) and ^{237}Np (right). See text for further explanations.

Two weighted averages of the three measurements are plotted in Figure 2. One using the corresponding ENDF evaluation for all the reference isotopes (red crosses) and one using the present data normalized to the ^{237}Np(n,f) data set and the ^{238}U(n,f) set (green stars). At the threshold region the two weighted averages are in agreement, and in concordance with the evaluations. Nevertheless, at the plateau region the weighted average using this experiment data maintains better the cross section shape and differs only by 2% with the ENDF/B-VII.1 evaluation. The data at the plateau region are in agreement with the values of Laptev (2004) and Staples (1998).

4.4. ^{242}Pu(n,f) cross section

Four measurements were performed to determine the ^{242}Pu(n,f) cross section. Two measurements were done without shielding using the ^{237}Np(n,f) and the ^{238}U(n,f) cross section. The other two measurements were done relative to the ^{235}U(n,f) cross section and using the shielding; one with a LiF neutron producing target and the other with a TiT. At the threshold region, the present results using different reference cross sections are in agreement with the evaluations up to 0.7 MeV. From this energy until 1.0 MeV the present results are around 5-10% lower than the evaluation. At the resonance-like peak structure visible in the evaluations at 1.0-1.1 MeV, the present results (either taken relative to ^{237}Np(n,f) or relative to ^{235}U(n,f)) are as well around 10% lower than evaluations. At the plateau region, the values obtained are systematically 5-7% lower than the evaluations, except for the data taken relative to the ^{235}U(n,f) cross section using a TiT target which are in agreement with the evaluations. At 1.6 MeV and 1.7 MeV the values obtained relative to ^{238}U(n,f) do not conserve the cross section shape, a similar effect was seen for the ratios ^{237}Np(n,f)/^{238}U(n,f) and the ^{240}Pu(n,f)/^{238}U(n,f).

In Figure 2 two weighted averages of the present data are plotted. The first one with all the data sets explained above normalized with the corresponding ENDF/B-VII.1 cross section (red crosses). The second one using, when possible, the present results for the ^{237}Np(n,f) and the ^{238}U(n,f) cross section (green stars). At threshold, the present experiment agrees with previous data sets and evaluations up to 0.7 MeV. From this energy to 1.5-1.6 MeV, the results are ≈10% lower than evaluations, without reproducing the resonance-like structure, but in agreement with the experiment of Staples (1998) and Tovesson (2009). At higher energies the second weighted average agrees with the present evaluations.

5. Conclusions

The neutron-induced fission cross section was measured for ^{240,242}Pu using a TFGIC at the Van de Graaff facility of the JRC-IRMM. The incident neutron energy covered the range between 0.3 and 3 MeV. Detailed studies of the efficiency of the measurement setup, the spontaneous fission half-lives of both ^{240,242}Pu and the neutron spectrum im-

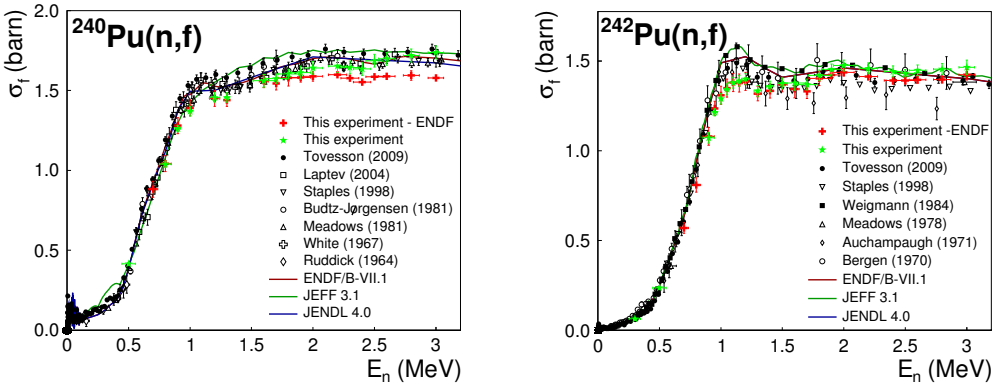

Fig. 2. Summary of the results achieved for the neutron-induced fission cross section of ^{240}Pu (left) and ^{242}Pu (right). See text for further explanations.

pinging the samples were performed to meet the target accuracy set out by the Nuclear Energy Agency. Measurements against three reference fission cross section reactions were performed, ^{237}Np(n,f), ^{235}U(n,f) and ^{238}U(n,f). In the case of the ^{240}Pu(n,f) cross section the present results are in agreement at the threshold region with evaluations, but at the plateau region the values are about 2% lower. For the ^{242}Pu(n,f) cross section, this experiment agrees at threshold only to 0.7 MeV, at higher energies the discrepancy reaches 10% with lower values than evaluations and, in any case the present data cannot confirm the resonance-like structure around 1.1 MeV. At energies above 1.5 MeV, the results are in agreement with previous experimental data and present evaluations. Additionally, results have been obtained for the ^{237}Np(n,f) and the ^{238}U(n,f) cross section.

Acknowledgements

The authors would like to acknowledge the technicians of the Van de Graaff accelerator (JRC-IRMM) for providing a very good beam. Additionally, one of the authors (P.S.-C.) acknowledges financial support from the ANDES collaboration (contract FP7 - 249671).

References

ANDES project, 2010. http://www.andes-nd.eu
Carlson, G. W., 1974. Nuclear Instruments and Methods 119, 97.
Chadwick, M. B., Herman, M., Obložinskỳ, P., *et al.*, 2011. Nuclear Data Sheets, vol. 112, 2887.
Lamphere R., 1956. Physical Review 104, 1654.
Laptev, A., Donets, A. Y., Fomichev, A., *et al.*, 2004. Nuclear Physics A734, E45.
Liskien, H. and Paulsen, A., 1973. Atomic Data and Nuclear Data Tables 11, 569.
Liskien, H. and Paulsen, A., 1975. Atomic Data and Nuclear Data Tables 15, 57.
MCNP. https://mcnp.lanl.gov/
Nakagawa, T., Shibata, K., Chiba, S., *et al.*, 1995. Journal of Nuclear Science and Technology 32, 1259.
Paradela, C., Tassan-Got, L., Audouin, L., *et al.*, 2010. Physical Review C 82, 034601.
Pommé, S., 2012, private communication.
ROOT. https://root.cern.ch/
Salvador-Castiñeira, P., Bryś, T., Eykens, R., *et al.*, 2013. Physical Review C 88, 064611.
Salvador-Castiñeira, P., Bryś, T., Hambsch, F.-J., *et al.*, 2014. Nuclear Data Sheets 119, 55.
Salvatores, M., 2008. NEA/WPEC-26, OECD.
Santamarina A., Bernard D., Blaise P., *et al.*, 2009. JEFF Report, vol. 22, no. 10.2, 2.
Sibbens, G., Moens, A., Eykens, R., *et al.*, 2014. Journal of Radioanalytical and Nuclear Chemistry 299, 1093.
Staples, P. and Morley, K., 1998. Nuclear Science and Engineering 129, 149.
Tovesson, F., Hill, T. S., Mocko, M., *et al.*, 2009. Physical Review C 79, 014613.